

PAPER • OPEN ACCESS

Design of a Planar Inverted F-Antenna for Medical Implant Communications Services Band

To cite this article: Sanaa Salama *et al* 2020 *J. Phys.: Conf. Ser.* **1711** 012001

View the [article online](#) for updates and enhancements.



IOP | ebooks™

Bringing together innovative digital publishing with leading authors from the global scientific community.

Start exploring the collection—download the first chapter of every title for free.

Design of a Planar Inverted F-Antenna for Medical Implant Communications Services Band

Sanaa Salama¹, Duaa Zyoud², Razan Daghlas³, and Ashraf Abuelhaija⁴

^{1,2,3} Telecommunication Engineering Department, Arab American University, Jenin, Palestine.

⁴ Electrical Engineering Department, AppliedScience Private University, Amman, Jordan.

Corresponding author's email address: sanaa.salama@aaup.edu

Abstract. A planar inverted F-implantable antenna is designed using the medical implant communications service (MICS) band (402–405MHz). The proposed antenna is designed using microstrip lines and short-circuited pin connecting between the ground plane and the patch. The total size of the proposed antenna is (24×32×2 mm³). The patch dimensions are (16×24 mm²). The calculated bandwidth at a return loss of -10 dB is 1MHz. The S-parameters, the near and far-fields, and the specific absorption rate (SAR) of the antenna is simulated and characterized. The design is carried out using CST Studio.

1. Introduction

Implantable antennas become essential in many medical applications such as: sugar level check, continuous real-time pressure measurements, endoscopy, insulin push out, and blood pressure measurements. Several frequency bands are being used for biomedical applications: The Medical Implant Communications Services (MICS) (402-405 MHz), the Industrial, Scientific, and Medical (ISM) bands, and the Wireless Medical Telemetry Service (WMTS) with the following frequency bands, [433.1-434.8 MHz], [608-614 MHz], [868-868.6 MHz], [902.8-928 MHz], [1395-1400 MHz], [1427-1432 MHz] and [2.4 -2.5 GHz]. The MICS allows ten channels with a bandwidth of 300KHz for each to support the operation of multiple implantable medical devices simultaneously, and minimizing interference with other services. The MICS band is more desired because it is available with a low power circuits, supports high data rate transmission, the used spectrum has a relatively low noise power, and it propagates well through human tissue [1]. The implantable antennas in the human body face many challenges as human body safety, miniaturization, efficiency, and bandwidth limitation. Due to size limitations in the human body, miniaturization becomes a significant key in the design of an implantable antenna. In [2-5], compact implantable antennas were proposed using different miniaturization techniques as meandered and spiral structures, cutting slots in the ground plane or in the patch to increase the current path and then size reduction will be obtained. In [6], a size reduction was obtained by choosing a high dielectric constant substrate. Bandwidth limitations in the design of implantable antennas were solved in [7,8], using different techniques as; monopole, dipole, and slot antennas. In [7], a combination of a monopole antenna and a C-shaped antenna was used to get a dual-band antenna, while in [8], a dipole antenna and a strip were combined for a dual resonance structure. Planar Inverted F antenna (PIFA) has been proposed by many groups [9-11] as implantable



antennas due to their advantages such as smaller size and omnidirectional far-field patterns. The PIFA antennas are recommended as implantable antennas because they are quarter-wavelength antennas, which make them good candidates for the small size applications. In [9], a compact broadband PIFA on Rogers 6010 substrate with a 10.2 dielectric constant was proposed. The antenna size is about 479 mm^3 , and the frequency bandwidth is 52 MHz. In [12], a size reduction was obtained by loading capacitive/inductive stubs. In addition, capacitive and inductive loads improve the matching at the desired frequency. In [13], a compact circularly polarized patch antenna working at 915MHz was proposed. The circularly polarized antenna is printed on Rogers 3010 with a dielectric constant of 10.2 and a loss tangent of 0.0035. Compact size was obtained by using loading stubs and meandering slots. In [14], a triple-band inserted miniaturized-slot PIFA was proposed. The suggested antenna has a volume of fewer than 1 cm^3 . The size reduction was achieved by optimizing the corresponding positions of the feed point and the use of short-circuited pins. While in [15], a PIFA omnidirectional antenna was suggested and focusing on the bandwidth enhancement by inserting several slits in the ground plane. An electrically small implantable antenna was proposed in [16] using MEMS technology. In [17], MEMS switches were used to design a reconfigurable antenna with differential feeding technique. A spiral implantable antenna shape in addition to the insertion of shorting pin were used in [18] to downsize the proposed antenna. The antenna was printed on Rogers 6010 substrate with a relative permittivity of 10.2. In addition, the ground plane was slotted for matching purposes.

2. The Design of the Implantable Antenna

The proposed antenna is a planar inverted F antenna designed on Rogers-RO3010 substrate of thickness 2mm and dielectric constant of 10.2; the ground plane dimensions are $24\text{mm} \times 32\text{mm}$. While the patch dimensions are $24\text{mm} \times 16\text{mm}$. The whole structure is shown in Figure 1. The antenna feed is made up of copper and extends between the ground plane and the patch. The short-circuited pin is connected between the patch and the ground plane and used for size reduction purposes. The simulated scattering parameter S_{11} is shown in Figure 2. A return loss of -22.018dB is obtained at 474.5 MHz and a frequency band of 1.47MHz at -10dB . The patch length in Figure 1 is 56 mm (calculated as the average between the inner and outer dimensions). The PIFA antenna is a quarter-wavelength antenna ($\lambda = 4 \times 56\text{mm} = 224\text{mm}$). Then the resonant frequency can be calculated as follows:

$$f = \frac{v_p}{\lambda} \quad (1)$$

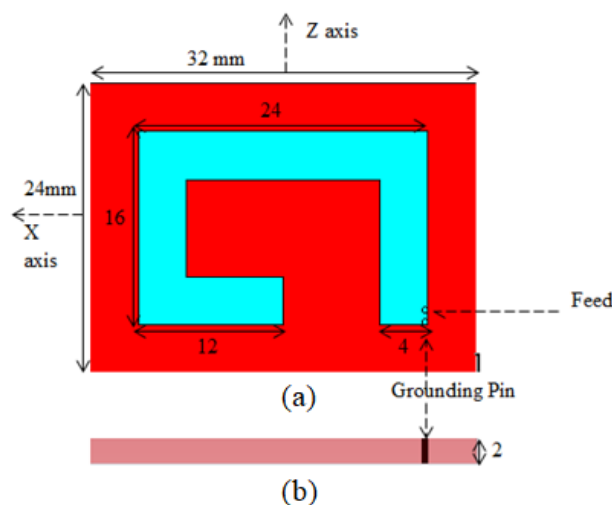


Figure 1. The structure of the proposed implantable PIFA. (a) Top view, and (b) side view. (one layer structure).

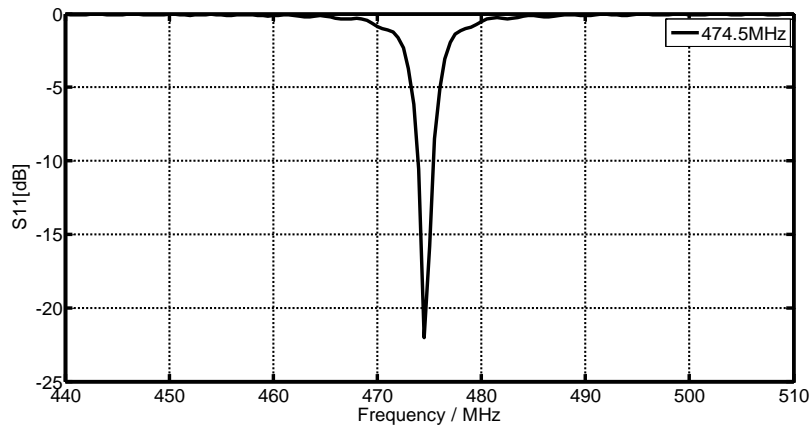


Figure 2.The simulated scattering parameter S11 of the implantable antenna before being implanted in the human skin.

where, v_p is the phase velocity ($3 \times 10^8 / \sqrt{\epsilon_r}$). Rogers-RO3010 substrate with $\epsilon_r = 10.2$ is used, then the calculated resonant frequency is 399.79MHz compared to 474.5MHz as the simulated results show. This difference between the calculated and simulated values of the resonant frequency is referred to as the short-circuited pin position with respect to the feed pin position. The resonant frequency increases as the short-circuited moves away from the feed pin. The proposed antenna resonant frequency lies outside the desired frequency band. The proposed antenna is then implanted in human skin with dimensions (36mm×28mm), and then the position of the short-circuited pin is optimized to be matched at 403MHz. Tissue electric properties in Table 1 are used to model the human skin. The antenna structure after being implanted in the human skin is shown in Figure 3. The corresponding simulated scattering parameter S11 is shown in Figure 4. Now after the PIFA is being implanted in the human skin, it resonates at 403MHz with a return loss of -21.77 dB and over a frequency band of 1MHz at -10dB. Also, the far-fields of the proposed antenna are simulated at 403MHz and presented in Figure 5 as a function of theta at constant phi of zero degrees (the elevation pattern) and as a function of phi at constant theta of 90 degrees (azimuth pattern). The antenna pattern is maximum directed away from the body. The antenna patterns in the azimuth plane ($\theta = 90$) are almost omnidirectional at 403 MHz. In contrast, in the elevation plane ($\phi = 0$), the antenna radiates approximately as a “figure of eight” at the desired frequency. The structure achieves a gain value of -18 dBi at 403 MHz. The near field (electric and magnetic) of the proposed antenna are shown in Figure 6.

Table 1. Electrical properties (permittivity, ϵ_r , conductivity, σ , loss tangent) of skin, muscle, and fat [18].

Biological tissues	MICS band			ISM band		
	ϵ_r	$\sigma(S/m)$	$\tan \delta$	ϵ_r	$\sigma(S/m)$	$\tan \delta$
Skin	46.7	0.69	0.79	38.1	2.27	0.33
Muscle	57.1	0.79	0.62	52.7	1.73	0.24
Fat	5.58	0.04	0.32	5.28	0.10	0.14

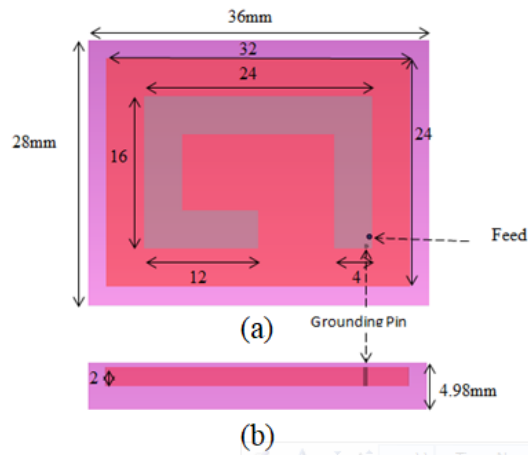


Figure 3.(a) Top view, and (b) side view of the implantable antenna after being implanted in the human skin (two layers of structure).

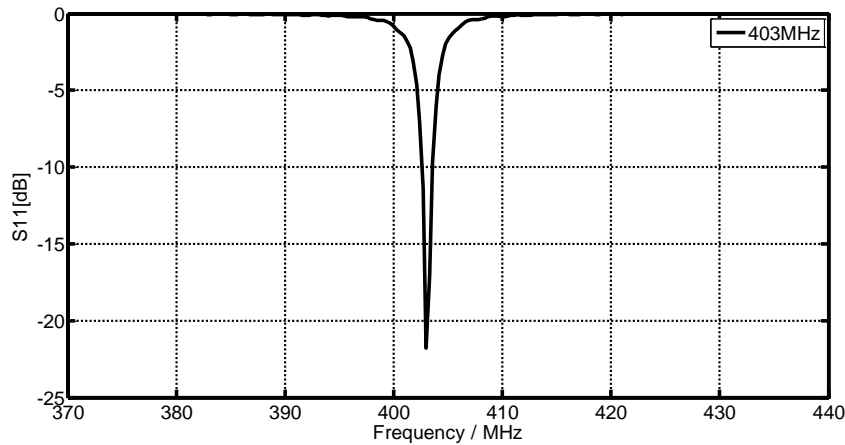


Figure 4.The simulated scattering parameter S11 of the implantable antenna after being implanted in the human skin.

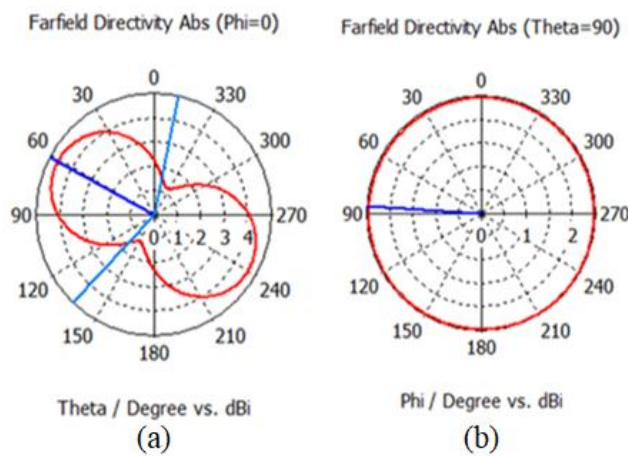


Figure 5. The radiation patterns of the proposed antenna after being implanted in the human skin at: (a) $\phi = 0^\circ$, and (b) $\theta = 90^\circ$.

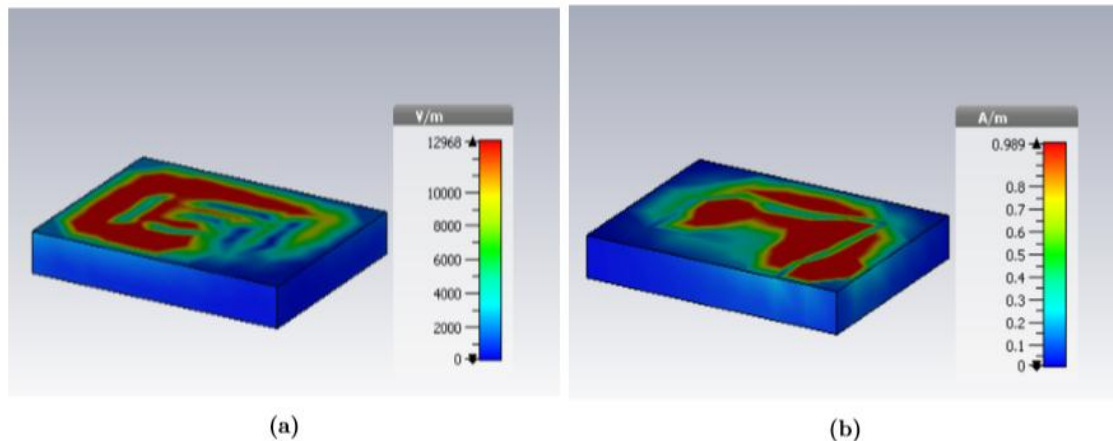


Figure 6. The near fields of the proposed antenna. (a) The electric field, and (b) the magnetic field.

3. Biocompatibility Considerations

In implantable antenna design, the biocompatibility issues have to be considered. Accordingly, there are two ways to ensure biocompatibility: the first one is to choose biocompatible materials such as Teflon, Macor, and Ceramic Alumina in the construction of the implantable antenna [19]. The second way is to cover the antenna with a thin layer of biocompatible material [20]. In this case, the thickness of the biocompatible material could affect the antenna characteristics. To prevent the direct contact of radiating patch with the human tissue, a Silicon superstrate with ($\epsilon_r = 3.1$, $\tan\delta = 0.0025$, and thickness 0.1mm) is used, which is a commonly used biocompatible material with low electrical loss. The simulated scattering parameter S_{11} of the structure, including the superstrate, is given in Figure 7. The resonant frequency of the implantable antenna after a Silicon superstrate is used becomes at 413.8MHz instead of 403MHz. To compensate for the frequency shift, the Silicon superstrate is replaced by an Alumina superstrate with ($\epsilon_r = 9.4$, $\tan\delta = 0.006$, and thickness 1mm). The resonant frequency after the Alumina superstrate is used becomes at 409.3MHz with a return loss of -27.62 dB. To adjust the resonant frequency to be at 403 MHz, the skin thickness is increased to be 6mm. The structure of the proposed implantable antenna after the Alumina superstrate is used shown in Figure 8. A return loss of -20.88 dB at 403MHz is obtained as Figure 9 shows. At an input power of 1 W, the SAR value at 403MHz is 148.39 W/kg for 1-g standard compared to the SAR value of 169.89 W/kg for the structure without a superstrate. To satisfy the safety restrictions, the maximum accepted input power should not be exceeded 10.78mW (1 g).

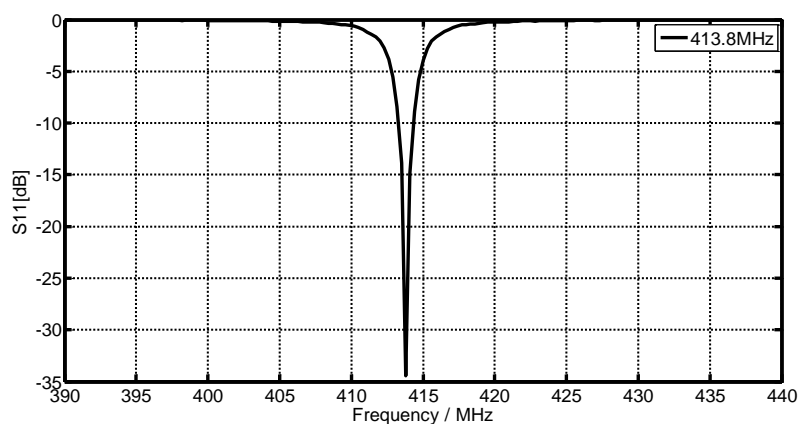


Figure 7. The simulated scattering parameter S_{11} of the implantable antenna after being implanted in the human skin and a Silicon superstrate is used.

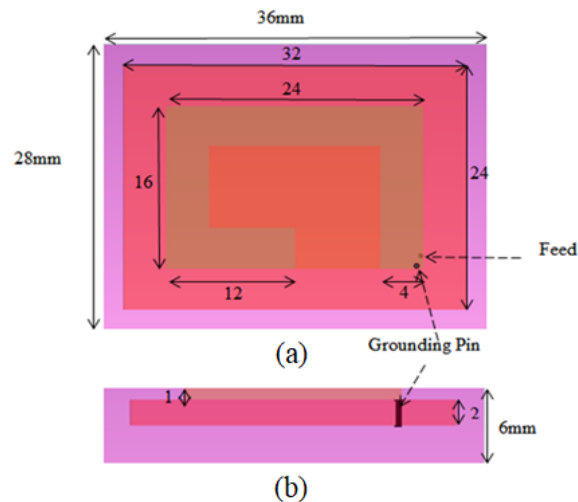


Figure 8. (a) Top view, and (b) side view of the implantable antenna after being implanted in the human skin and an Alumina superstrate is used.(three layers of structure).

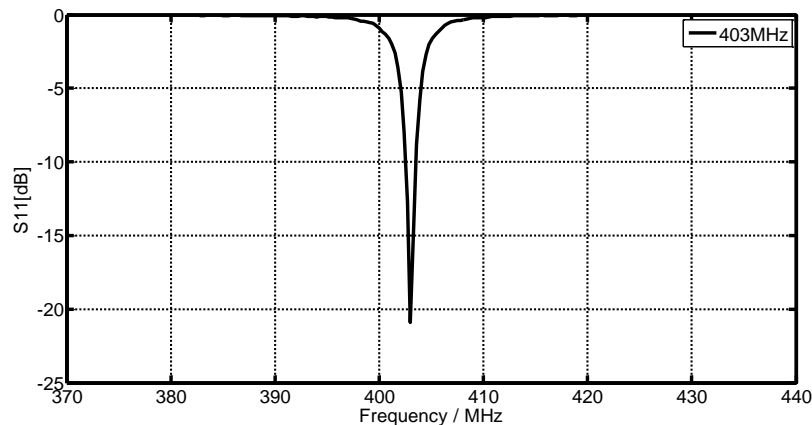


Figure 9. The simulated scattering parameter S_{11} of the implantable antenna after being implanted in the human skin and an Alumina superstrate is used.

4. Conclusion

In this work, a planar inverted-F implantable antenna is designed for the MICS band. The proposed antenna is resonating at 403MHz and covers a frequency band of 1MHz at -10dB. The structure is designed and simulated using CST studio. The SAR is evaluated at 403MHz for 1g standard, and the input power should be reduced to 10.78mW mW to satisfy the safety restrictions at the desired frequency. For the proposed antenna, a return loss of -21.77 dB is obtained at 403 MHz. In addition, an omniradiation pattern in the azimuth plane and a figure of eight pattern in the elevation plane is obtained.

References

- [1] A. Kiourti and K. S. Nikita, "Performance of Miniature Implantable Antennas for Medical Telemetry at 402, 433, 868 and 915 MHz", *Wireless Mobile Communication and Healthcare*, 2013, pp. 122-129.
- [2] J. Kimi, Y. Rahmat-samii, "Planar InvertedF Antennason Implantable Medical Devices: Meandered Type Versus Spiral Type", *Microw. Opt. Technol. Letter*, 2006, 48, pp. 567–572.
- [3] C. R. Liu, Y. X. Guo, S. Q. Xiao, "A Hybrid Patch/Slot Implantable Antenna for Biotelemetry Devices", *IEEE Antennas Wirel. Propag. Letter*, 2012, 11, pp. 1646–1649.

- [4] R. Q. Li, S. Q. Xiao, "Compact Slotted Semi-Circular Antenna for Implantable Medical Devices", *Electron. Letter*, 2014, 50, pp. 1675–1677.
- [5] H. Li, Y.-X. Guo, and S.-Q. Xiao, "Broadband Circularly Polarized Implantable Antenna for Biomedical Applications," *Electronics Letters*, 2016, vol.52,no.7,pp.504–506.
- [6] A. Damaj , S. Abou Chahine and I. Damaj, "The Design and Implementation of Electrically Small Reconfigurable Patch Antennas.," in *GCC Conference and Exhibition (GCC)*, 2011.
- [7] C. L. Tsai, K. W. Chen, and C. L. Yang, " Implantable Wideband Low-SAR Antenna with C-Shape Coupled Ground", *IEEE Antennas Wirel. Propag. Letter*, 2015, 14, pp. 1594–1597.
- [8] L. J. Xu, Y. X. Guo, and W.Wu, "Bandwidth Enhancement of an Implantable Antenna", *IEEE Antennas Wirel. Propag. Letter*, 2015, 14, pp. 1510–1513.
- [9] R. Li, B. Li, G. Du, X. Sun, and H. Sun, " A Compact Broadband Antenna with Dual-Resonance for Implantable Devices", *Micromachines*, 2019, 59, 10.
- [10] J. Kim and Y. Rahmat-Samii, "Implanted Antennas Inside a Human Body: Simulations, Designs, and Characterizations," *IEEE Transactions on Microwave Theory and Techniques*, 2004, vol. 52, no. 8, pp.1934–1943.
- [11] C.M. Lee, T.C. Yo, F.J. Huang, and C.H. Luo, "Dual-Resonant π -Shape with Double L-Strips PIFA for Implantable Biotelemetry," *Electronics Letters*, 2008, vol.44,no.14,pp.837–839.
- [12] C. Liu, Y. X. Guo, and S. Xiao, "Capacitively Loaded Circularly Polarized Implantable Patch Antenna for ISM Band Biomedical Applications," *IEEE Transactions on Antennas and Propagation*, 2014, vol.62,no.5,pp.2407–2417.
- [13] K. Zhang, C. Liu, X. Liu, H. Guo, and X. Yang, "Miniaturized Circularly Polarized Implantable Antenna for ISM-Band Biomedical Devices," *International Journal of Antennas and Propagation*, 2017, pp.1-9.
- [14] G. Farhad and A. S. Mohan, "Miniaturized Slot PIFA Antenna for Triple-Band Implantable Biomedical Applications," in *IEEE MTT-S International*, 2013.
- [15] S. Shaheen, S. Dharanya, V. Divya, and A. Umamakeswari, "Design of PIFA Antenna for Medical Applications," *International Journal of Engineering and Technology (IJET)*, 2013, vol. 5, pp. 127-132.
- [16] F. J. O. Rodrigues, L. M. Gonçalves and P. M. Mendes, "Electrically Small and Efficient on-Chip MEMS Antenna for Biomedical Devices," in *Antenna Technology (IWAT)*, 2010.
- [17] S. Bhattacharjee, S. Maity, S. K. Metya, and C. T. Bhunia, "Performance Enhancement of Implantable Medical Antenna Using differential Feed Technique," *Engineering Science and Technology, an International Journal*, 2016, 19(1), pp.642–650.
- [18] A. Basir, A. Bouazizi, M. Zada, A. Iqbal, S. Ullah, and U. Naeem, "A Dual-Band Implantable Antenna with Wide-Band Characteristics at MICS and ISM Bands," *MicrowOpt Technol Lett.*, 2018, pp. 1-5.
- [19] P. Soontornpipit, C. M. Furse, and Y. C. Chung, "Design of Implantable Microstrip Antenna for Communication with Medical Implants," *IEEE Transactions on Microwave Theory and Techniques*, 2004, vol.52,no.8,pp.1944–1951.
- [20] T. Karacolak, R. Cooper, J. Butler, S. Fisher, and E. Topsakal, "In vivo Verification of Implantable Antennas Using Rats as Model Animals," *IEEE Antennas and Wireless Propagation Letters*, 2010, vol. 9, pp.334–337.